

1           **Title: A *Trypanosoma cruzi* Trans-Sialidase Peptide Demonstrates High**  
2           **Serological Prevalence Among Infected Populations Across Endemic Regions**  
3           **of Latin America**

4  
5           **Authors:** Hannah M. Kortbawi<sup>1,2†</sup>, Ryan J. Marczak<sup>3,4‡</sup>, Jayant V. Rajan<sup>1‡</sup>, Nash L. Bulaong<sup>5</sup>,  
6           John E. Pak<sup>5</sup>, Wesley Wu<sup>5</sup>, Grace Wang<sup>5</sup>, Anthea Mitchell<sup>5</sup>, Aditi Saxena<sup>5§</sup>, Aditi  
7           Maheshwari<sup>3,4||</sup>, Charles J. Fleischmann<sup>4¶</sup>, Emily A. Kelly<sup>4</sup>, Evan Teal<sup>4</sup>, Rebecca L. Townsend<sup>6</sup>,  
8           Susan L. Stramer<sup>6††</sup>, Emi E. Okamoto<sup>7#</sup>, Jacqueline E. Sherbuk<sup>7\*\*</sup>, Eva H. Clark<sup>8,9</sup>, Robert H.  
9           Gilman<sup>10</sup>, Rony Colanzi<sup>11</sup>, Efstathios D. Gennatas<sup>3,12</sup>, Caryn Bern<sup>3\*</sup>, Joseph L. DeRisi<sup>1,5\*</sup>,  
10          Jeffrey D. Whitman<sup>4\*</sup>

11           **Affiliations:**

12           <sup>1</sup>Department of Biochemistry and Biophysics, University of California San Francisco; San  
13           Francisco, CA, USA.

14           <sup>2</sup>Medical Scientist Training Program, University of California San Francisco; San Francisco, CA,  
15           USA.

16           <sup>3</sup>Department of Epidemiology and Biostatistics, University of California San Francisco; San  
17           Francisco, CA, USA.

18           <sup>4</sup>Department of Laboratory Medicine, University of California, San Francisco; San Francisco,  
19           CA, USA.

20           <sup>5</sup>Chan Zuckerberg Biohub San Francisco; San Francisco, CA, USA.

21           <sup>6</sup>Scientific Affairs, American Red Cross; Gaithersburg, MD, USA.

22           <sup>7</sup>New York University School of Medicine; New York, NY, USA.

23           <sup>8</sup>Section of Infectious Diseases, Department of Medicine, Baylor College of Medicine; Houston,  
24           TX, USA.

25           <sup>9</sup>Division of Tropical Medicine, Department of Pediatrics, Baylor College of Medicine; Houston,  
26           TX, USA.

27           <sup>10</sup>Johns Hopkins University Bloomberg School of Public Health; Baltimore, MD, USA.

28           <sup>11</sup>Universidad Catolica Boliviana; Santa Cruz, Plurinational State of Bolivia.

29           <sup>12</sup>Department of Medicine, University of California San Francisco; San Francisco, CA, USA.

30           †, Authors contributed equally.

31           ‡, JVR current affiliation, Current affiliation Pfizer, Inc; Collegeville, PA, USA.

32           §, AS current affiliation, Department of Immunology and Infectious Diseases, Harvard T. H.  
33           Chan School of Public Health; Boston, MA, USA.

34           ||, AM current affiliation, Keck School of Medicine, University of Southern California, Los  
35           Angeles, CA, USA.

36           ¶, CJF current affiliation, Noorda College of Osteopathic Medicine; Provo, UT, USA.

37 #, EEO current affiliation, Independent Consultant.

38 \*\*, JES current affiliation, University of South Florida; Tampa, FL, USA.

39 ††, SLS current affiliation, Infectious Disease Consultant, North Potomac, MD

40 \*, Corresponding authors, [caryn.bern2@ucsf.edu](mailto:caryn.bern2@ucsf.edu), [joe@derisilab.ucsf.edu](mailto:joe@derisilab.ucsf.edu),

41 [jeffrey.whitman@ucsf.edu](mailto:jeffrey.whitman@ucsf.edu).

42 **One Sentence Summary:** Phage display immunoprecipitation sequencing (PhIP-seq) designed  
43 with a *T. cruzi* whole proteome library reveals a trans-sialidase peptide antigen (TS-2.23) with  
44 antibody responses highly prevalent across endemic regions of Latin America.

45 **Abstract:** Infection by *Trypanosoma cruzi*, the agent of Chagas disease, can irreparably damage  
46 the cardiac and gastrointestinal systems during decades of parasite persistence and related  
47 inflammation in these tissues. Diagnosis of chronic disease requires confirmation by multiple  
48 serological assays due to the imperfect performance of existing clinical tests. Current serology  
49 tests utilize antigens discovered over three decades ago with small specimen sets predominantly  
50 from South America, and lower test performance has been observed in patients who acquired *T.*  
51 *cruzi* infection in Central America and Mexico. Here, we attempt to address this gap by  
52 evaluating antibody responses against the entire *T. cruzi* proteome with phage display  
53 immunoprecipitation sequencing comprised of 228,127 47-amino acid peptides. We utilized  
54 diverse specimen sets from Mexico, Central America and South America, as well as different  
55 stages of cardiac disease severity, from 185 cases and 143 controls. We identified over 1,300  
56 antigenic *T. cruzi* peptides derived from 961 proteins between specimen sets. A total of 67  
57 peptides were reactive in 70% of samples across all regions, and 3 peptide epitopes were  
58 enriched in  $\geq 90\%$  of seropositive samples. Of these three, only one antigen, belonging to the  
59 trans-sialidase family, has not previously been described as a diagnostic target. Orthogonal  
60 validation of this peptide demonstrated increased antibody reactivity for infections originating  
61 from Central America. Overall, this study provides proteome-wide identification of seroreactive  
62 *T. cruzi* peptides across a large cohort spanning multiple endemic areas and identified a novel  
63 trans-sialidase peptide antigen (TS-2.23) with significant potential for translation into diagnostic  
64 serological assays.

65 **Main Text:**

## 66 INTRODUCTION

67 Chagas disease is caused by infection with the protozoan parasite, *Trypanosoma cruzi*, which is  
68 transmitted by triatomine insect vectors. The disease is endemic to the Americas, with vector-  
69 borne transmission occurring in suitable ecological zones of Latin America (1). In the United  
70 States (US), the major disease burden occurs among Latin American immigrant populations  
71 exposed in their birth countries, although rare autochthonous infections have been documented in  
72 Texas, California, Arizona, Tennessee, Mississippi and other southern states (2, 3). Chronic  
73 Chagas disease is considered a lifelong infection without treatment. *T. cruzi* can infect many  
74 nucleated cell types but causes pathology in the cardiac and gastrointestinal systems. An  
75 estimated 20 to 30% of people with chronic Chagas disease develop symptoms of end organ  
76 damage after years to decades of infection. Related cardiac presentations include cardiac  
77 conduction system deficits, dilated cardiomyopathy, and sudden cardiac death (4). Ten percent of  
78 infected individuals may develop gastrointestinal dysmotility disorders (5, 6). Because this  
79 parasite is predominantly intracellular in the chronic phase and symptoms are largely non-

80 existent or non-specific, detection of anti-*T. cruzi* antibodies in peripheral blood is the most  
81 sensitive method for diagnosis and is the only reliable means of screening asymptomatic patients.

82 The test performance of current Chagas disease serology assays does not have the accuracy  
83 (sensitivity or specificity) to effectively diagnose patients by one test alone (7). Pan American  
84 Health Organization/World Health Organization (PAHO/WHO) guidelines require confirmation  
85 by two tests with distinct antigen sources. The indications for *T. cruzi* serology span many areas  
86 of healthcare, including clinical diagnosis, blood donor screening, and solid organ or  
87 hematopoietic stem cell transplant donor and recipient testing (8-11). In practice, securing repeat  
88 testing for patients and identifying clinical laboratories that offer more than one serology test can  
89 be difficult and time consuming, and ultimately patients may be lost to follow-up. Given the  
90 mounting awareness of the need for Chagas disease screening and imperfect test performance, it  
91 is clear that the serology assays themselves must be improved to increase the effectiveness of  
92 screening and diagnosis efforts.

93 Recent studies evaluating regionally-diverse Chagas disease populations highlight differential  
94 reactivity to commercial *T. cruzi* serology assays between infected populations; with the lowest  
95 reactivity in individuals from Mexico, intermediate reactivity from Central America, and the  
96 highest reactivity from South America (12-15). Up to an estimated 10% loss in sensitivity  
97 between infections originating from Mexico compared to South America has been observed  
98 depending on the assay used (12). Other studies based in endemic areas have documented  
99 decreased performance of commercial serological assays in regions of Mexico and Central  
100 America, as well as Peru (16-19). *T. cruzi* is a genetically diverse parasite, currently classified  
101 into six genetic lineages or discrete typing units (DTUs: TcI – TcVI) (20), plus a potential  
102 seventh, bat-associated genotype (TcBat), most closely related to TcI (21). It is hypothesized that  
103 host immunological responses and antigenic differences between regional *T. cruzi* strains may be  
104 the basis of the differential serological responses. However, the areas with problematically low  
105 reactivity to commercial assays are largely found where TcI is predominant, but not all TcI-  
106 predominant areas show low reactivity (22). Genetic variation is also high within TcI (23),  
107 suggesting that DTU-level classification is not sufficiently granular to map host immunology to  
108 parasite genetics.

109 The antigens used in current commercial diagnostics originated from a surge of Chagas disease  
110 serology research over the last three decades (24). These studies tended to rely on screening with  
111 sera from high prevalence regions of South America, where TcII/V/VI are predominant; mainly  
112 Brazil and Argentina. Since then, more robust techniques for antigen discovery have emerged in  
113 the form of high-density peptide microarrays. Recent application of these techniques to Chagas  
114 disease have generated additional antigen targets (25-27). However, these studies used pooled  
115 sera for determining the initial down selection of antigenic targets for secondary peptide array  
116 libraries. Such an approach is unable to discern commonality of antigens across the entire *T.*  
117 *cruzi* proteome among the pooled sera. The antigen targets chosen for follow-on validation in  
118 individual specimens were therefore biased towards the highest reactivity antigens within a pool,  
119 not necessarily the highest prevalence antigens.

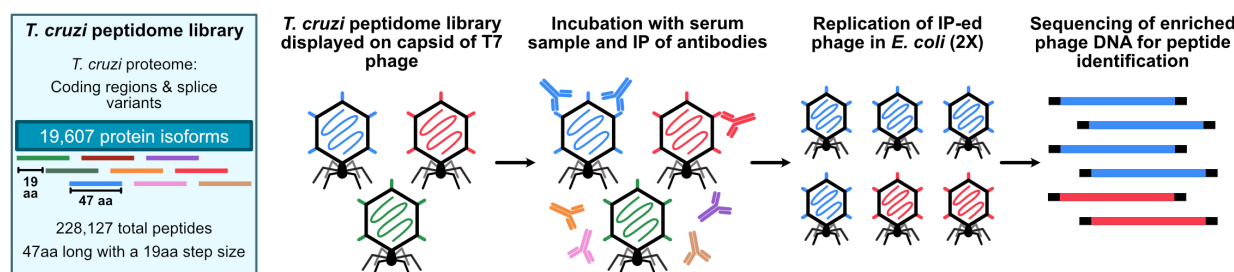
120 To address these gaps, we employed phage display immunoprecipitation sequencing (PhIP-seq)  
121 (28) using a synthetic oligonucleotide library with high-density coverage of the *T. cruzi*  
122 proteome using 47 amino acid peptides. We performed immunoprecipitation using 185 serology-  
123 confirmed cases from geographically diverse regions of Latin America to explicitly represent the  
124 genetic diversity of *T. cruzi* antigens across DTUs, as well as varying presentations of Chagas

125 cardiomyopathy to control for any differences by disease severity. The goal of this study was to  
126 employ a next-generation antigen discovery technique to *T. cruzi* and evaluate high-prevalence  
127 antigen targets with translational potential for serological diagnostics.

## 128 RESULTS

### 129 Development of *T. cruzi* proteome library

130 We constructed a T7 phage-display library to display the entire *T. cruzi* CL Brener proteome in  
131 49-amino acid (aa) peptides with a 19-mer overlap in consecutive sequences (*Materials and*  
132 *Methods*, Fig. 1). The library includes 228,127 *T. cruzi* peptides that represent 19,607 proteins.  
133 Over 99.6% of the ordered peptides were represented in the final cloned library, with 90% of  
134 peptides represented within a 9-fold difference of read counts (Fig. S1).



135  
136 **Fig. 1. PhIP-seq library design and assay steps.** Phage library displays the proteome of *T.*  
137 *cruzi* in 47-aa peptides with a 19-aa step size on the capsid of T7 phage. The library  
138 includes all coding regions of the proteome and splice variants. We performed the PhIP-  
139 seq assay by incubating the phage library with human plasma, followed by  
140 immunoprecipitation of antibodies in the sample and enrichment of antibody-bound  
141 phage through lysis in *E. coli*. We performed two rounds of enrichment and then  
142 sequenced the enriched phage to obtain the identity of the immunoprecipitated peptides.

### 143 PhIP-seq identifies antibodies to *T. cruzi* peptides

144 We performed PhIP-seq on peripheral blood samples from three distinct specimen sets including  
145 US blood donors with routine Chagas disease serology screening (BD,  $n=90$ ;  $n=64$  seropositive,  
146  $n=26$  seronegative), a Chagas disease cardiac biomarker study (CBM,  $n=143$ ;  $n=121$   
147 seropositive,  $n=22$  seronegative), and independent healthy controls (NYBC,  $n=95$ ). See  
148 *Materials and Methods* for a full description of these specimens. The PhIP-seq library contained  
149 human GFAP sequences, so a polyclonal anti-GFAP antibody was used as a positive control for  
150 immunoprecipitation. Positive control samples were highly enriched for GFAP peptides (Fig.  
151 S2). We excluded ten samples from the analysis due to low sequencing read counts; seven  
152 seropositive CBM samples, two seronegative CBM study samples, and one NYBC control. In  
153 total, 185 cases and 143 controls were included for further data analysis.

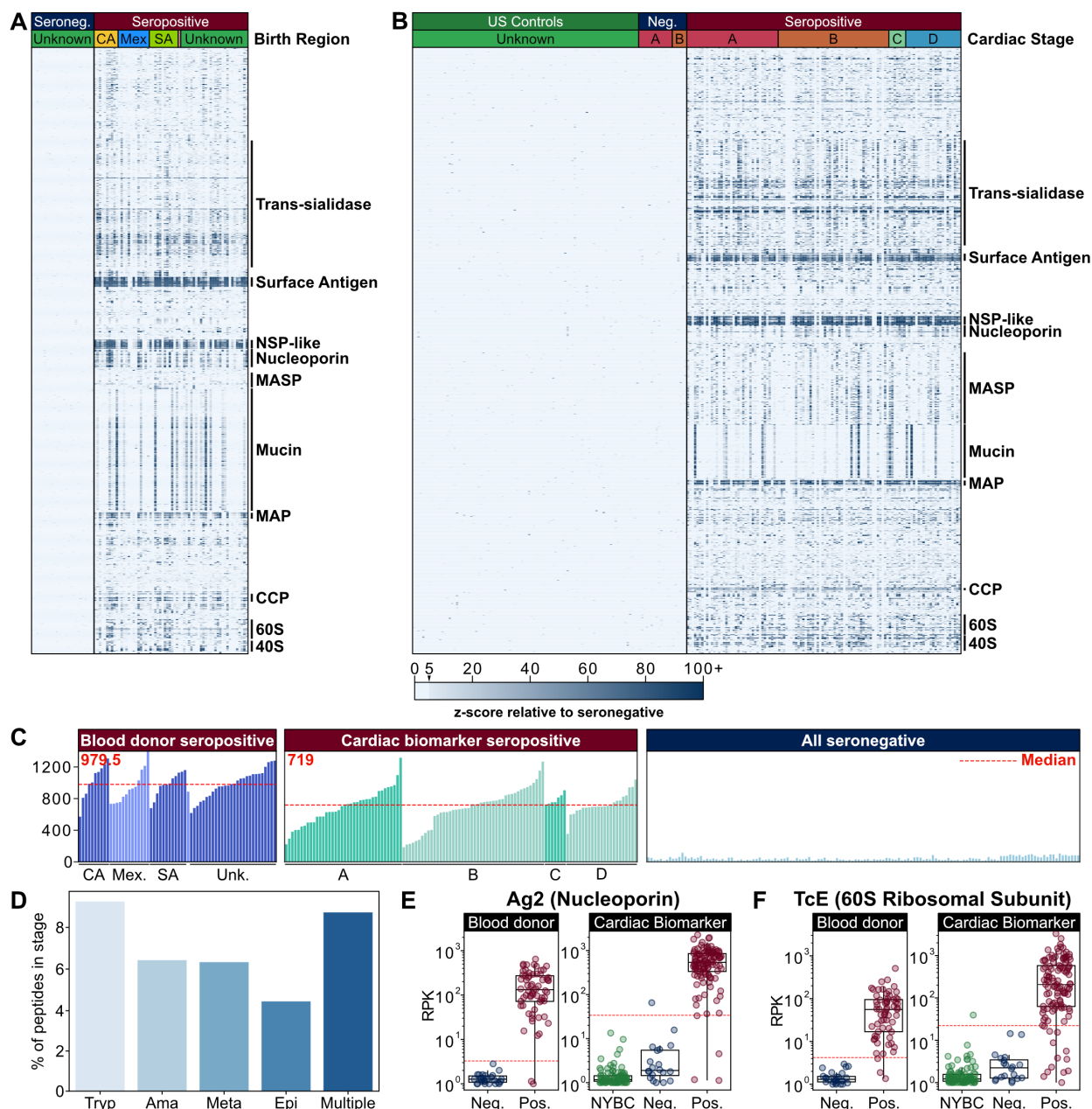
154 We used a conservative analysis approach to identify antibody reactivity to individual *T. cruzi*  
155 peptides that were enriched ( $z$ -score  $\geq 5$ ) in at least 5% of seropositive patients (Fig. S3).  $Z$ -  
156 scores were calculated based on the distribution of sequencing reads per 100,000 (RPK) value  
157 for a given peptide in seronegative patients, which included endemic region seronegative  
158 controls as well as independent seronegative controls from the US. With this approach, 5,638  
159 individual peptides representing 4,001 proteins were enriched in the seropositive CBM samples,  
160 and 8,710 peptides representing 5,629 proteins were enriched in the seropositive BD samples.

161 Between both cohorts, 12,978 antigenic peptides corresponding to 7,373 unique proteins were  
162 identified, with an overlap of 1,370 peptides across 961 proteins in both Chagas disease study  
163 sets (Fig. S4). A total of 67 and 85 peptides were reactive in at least 70% of samples among the  
164 BD samples and CBM samples, respectively. Across both cohorts, 43 of these 70% seroreactivity  
165 peptides were shared.

### 166 **Significantly enriched *T. cruzi* antigens in seropositive samples**

167 The antigenic peptides identified across both specimen sets represented 38% of the 19,607-  
168 member proteome of *T. cruzi*. Most of these peptides demonstrated no enrichment in  
169 seronegative samples (Fig. 2a, b). The median number of enriched Chagas disease-specific  
170 peptides in each seropositive sample was higher in the BD specimens compared to the CBM  
171 specimens (Fig. 2c), but the mean number of enriched peptides per sample did not significantly  
172 differ within cohorts by patient region of origin (BD specimens) or by heart disease stage (CBM  
173 specimens) (Kruskall-Wallis, BD  $H(2) = 1.77, p = 0.41$ ; CBM  $H(3) = 2.49, p = 0.48$ ).

174 The proteins from which the enriched peptides derive are predominantly expressed in the host  
175 phase lifecycle stages of *T. cruzi* (metacyclic trypomastigotes, trypomastigotes, and amastigotes)  
176 (29) (Fig. 2d). There were relatively fewer seroreactive peptides that corresponded to proteins  
177 expressed in the epimastigote form, which only occurs in the gut of the triatomine vector.  
178 Examples of host phase-specific proteins that had high antibody reactivity included trans-  
179 sialidases and mucin-associated surface proteins.



180  
 181 **Fig. 2. PhIP-seq captures known antigens across the *T. cruzi* life cycle stages. (A,B)** Heatmap  
 182 of z-score enrichment over seronegative controls in the (A) blood donor (BD) specimens  
 183 (n=64 seropositive, n=26 seronegative) and the (B) cardiac biomarker (CBM) specimens  
 184 (n=114, seropositive; n=18, seronegative; n=95, healthy controls) for seroreactive  
 185 peptides (rows) with >15% seropositivity within each cohort. Peptides are sorted by  
 186 protein name and samples are sorted by patient region of origin (n=10, Central America  
 187 [yellow]; n=13, Mexico [blue]; n=12, South America [light green]; n=1, USA [pink];  
 188 n=28, unknown [green]) (A), or cardiac disease stage (n=14 stage A seronegative  
 189 [magenta]; n=6 stage B seronegative [orange]; n=38 stage A seropositive [magenta];  
 190 n=46 stage B seropositive [orange]; n=7 stage C seropositive [light green]; n=23 stage D  
 191 seropositive [blue]) (B). Protein groups with well-characterized antigens are indicated by  
 192 labels (Surface antigen, Surface antigen 2 (CA-2); NSP-like, Nucleoporin NSP1-like C-

193 terminal domain-containing protein; MASP, Mucin-associated surface protein; Mucin,  
194 TcMUCII; MAP, Microtubule-associated protein; CCP, Calpain-like cysteine peptidase;  
195 60S, 40S, ribosomal subunit proteins). (C) Breadth of antibody reactivity, shown as the  
196 number of seroreactive peptides in each person. The dotted red line and number signify  
197 the median number of seroreactive peptides in BD and CBM specimen sets. Samples are  
198 grouped by geographic region (BD specimens) and heart disease stage (CBM specimens).  
199 (D) Number of peptides identified as seroreactive in this study that are part of proteins  
200 expressed in specific stages of the *T. cruzi* life cycle (Tryp = trypomastigote; Ama =  
201 amastigote; Meta = metacyclic trypomastigote; Epi = epimastigote; Multiple = protein is  
202 expressed in trypomastigote, amastigote, and/or metacyclic trypomastigote stages). Stage  
203 expression analysis shows seroreactive peptides in every host-interfacing lifecycle stage.  
204 Stage-specific expression is based on the ‘Life cycle proteome (Brazil)’ data set from  
205 TriTrypDB. Gene IDs for stage-specific proteins were mapped onto the gene IDs that  
206 corresponded to seroreactive peptides. (E,F) Selected known seroreactive antigens are  
207 captured by *T. cruzi* PhIP-seq. Neg. is seronegative specimens from the respective  
208 specimen sets; Pos. is seropositive specimens from the respective cohorts; NYBC is  
209 NYBC US controls. Antibody reactivity to two known antigens (E) Ag2, a nucleoporin  
210 protein, and (F) TCE, a 60S ribosomal subunit protein are plotted as reads per 100,000  
211 (RPK). The dotted red line signifies the RPK that corresponds to a z-score cutoff of 5 in  
212 the seronegative population of each cohort.

### 213 **Identification of high-prevalence *T. cruzi* antigens across Latin America**

214 To identify high-prevalence antigens shared across endemic regions representing different *T.*  
215 *cruzi* DTUs, we first analyzed BD specimens, which included individuals born in Mexico,  
216 Central America and South America. We performed two complementary approaches to identify  
217 individual antigens with sufficient seroprevalence to have utility for clinical diagnostic assays.  
218 First, we used the z-scored, peptide-level data to identify peptides enriched in  $\geq 90\%$  of  
219 seropositive BD samples. Second, we used mass univariate analysis to create a ranked list of top  
220 antigenic peptides by largest predictor coefficient values. The mass univariate analysis approach  
221 models peptide RPK scores based on diagnostic status in our BD specimens. All peptides  
222 identified by the z-score approach were also identified as significantly enriched by the mass  
223 univariate analysis (Fig. S5). These analyses were then performed on the CBM specimens to  
224 evaluate for any differences in high-prevalence antigens by cardiac disease status; none were  
225 identified.

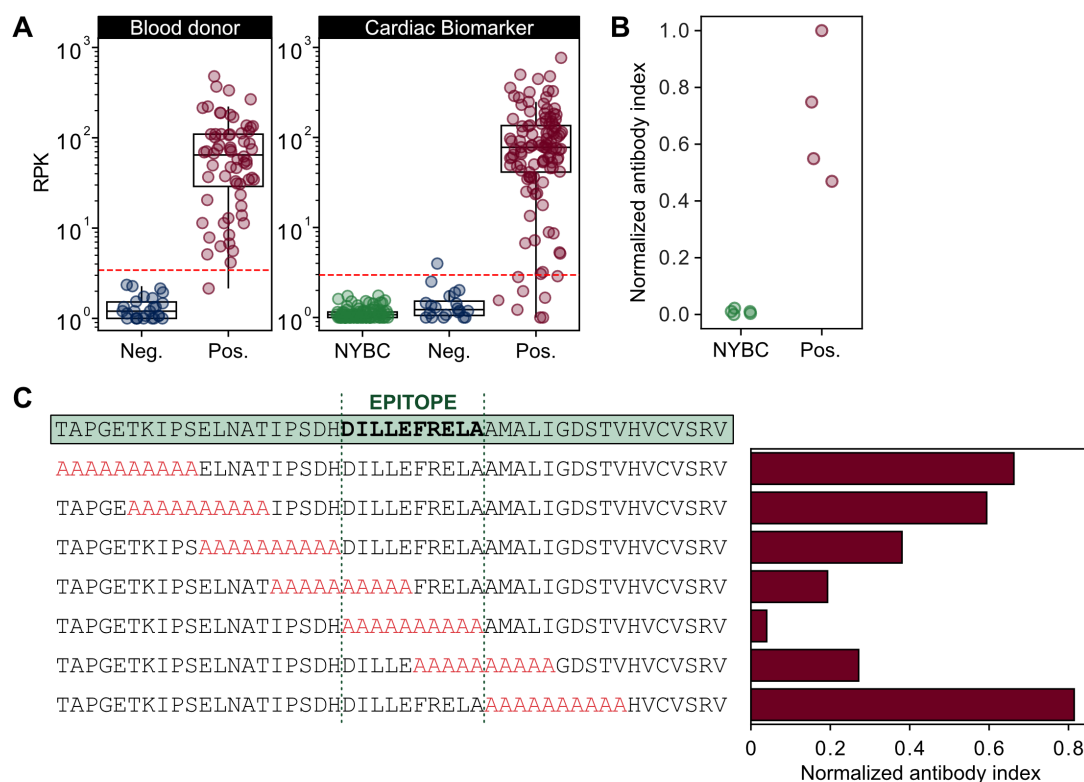
226 These analyses yielded 23 peptides (Table S1), including 20 peptides that all contain the  
227 repetitive PFGQAAAGDKPS antigenic sequence, present in a current diagnostic antigen known  
228 as Ag 2 (30, 31) (Fig. 2e). An additional highly reactive peptide, which contained the antigenic  
229 sequence KAAAPKKAAAPQ, has high sequence homology to another known diagnostic  
230 antigen, TcE (32) (Fig. 2f). The final two high-prevalence peptides belonged to the trans-  
231 sialidase family (Fig. 3a) and shared the sequence  
232 APGETK[V/I]PSELNATIPSDHDILLEFR[D/E]LAAMALIG. To our knowledge, this peptide is  
233 novel as a diagnostic antigen candidate.

### 234 **Epitope mapping and validation of the high-prevalence trans-sialidase antigen**

235 To orthogonally validate antibody reactivity to the high-prevalence trans-sialidase peptide, we  
236 performed a split-luciferase binding assay (SLBA). Briefly, we generated the trans-sialidase

237 peptide with a C-terminal HiBiT tag and immunoprecipitated it with plasma from 4 seropositive  
 238 BD patient samples with the highest PhIP-seq RPK values and five independent healthy US  
 239 controls. Incubation of the immunoprecipitated peptides with LgBiT produces luminescence as a  
 240 quantitative measurement of antibody binding. Four Chagas disease seropositive samples with  
 241 high PhIP-seq enrichment were reactive to the trans-sialidase peptide, while seronegative control  
 242 samples were not (Fig. 3b).

243 A sequential alanine-scan was performed to further map the reactive epitope of the trans-  
 244 sialidase peptide. Using samples from 5 seropositive BD patients, we determined that the critical  
 245 region for immunoreactivity was a ten aa sequence that spans positions 648 to 658 of the full-  
 246 length trans-sialidase protein (DILLEFRELA) (Fig. 3c). To be permissive of the epitope we  
 247 chose a final antigenic sequence of IPSDHDILLEFRELA, corresponding to the two alanine  
 248 blocks with the lowest reactivity, henceforth be referred to as TS-2.23. Basic local alignment  
 249 search tool (BLAST) analysis of TS-2.23 in NCBI database identified 37 proteins from all *T.*  
 250 *cruzi* entries with >93% (15-aa) sequence identity, all of which were from trans-sialidase or  
 251 putative trans-sialidase genes.



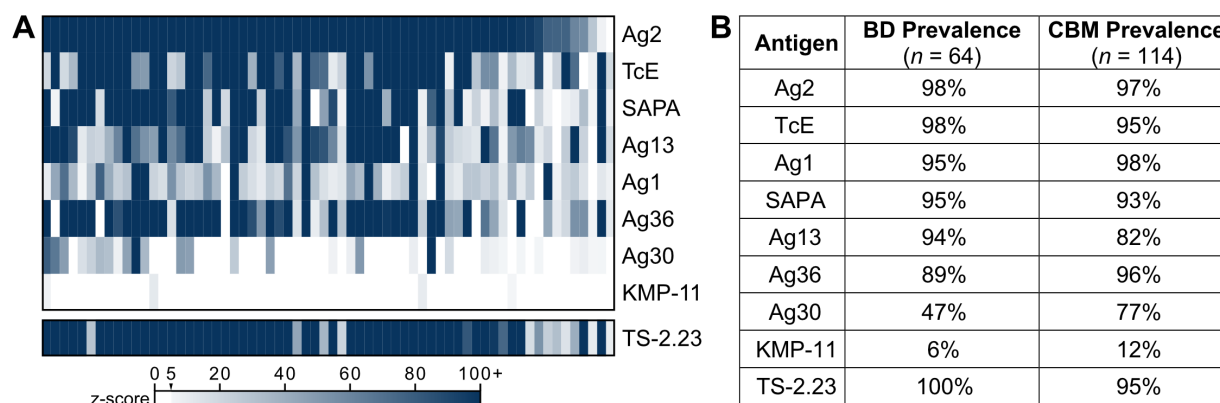
252  
 253 **Fig. 3. A novel trans-sialidase peptide sequence is a highly reactive serological antigen.** (A)  
 254 Anti-trans-sialidase peptide antibody reactivity is plotted as RPK. The dotted red line  
 255 signifies the RPK that corresponds to a z-score cutoff of 5 in the seronegative population  
 256 of each cohort. (B) Trans-sialidase reactivity orthogonal validation using a split-  
 257 luciferase binding assay (SLBA). Reactivity was tested against four seropositive blood  
 258 donor specimens and five seronegative US healthy control specimens. (C) Alanine-  
 259 scanning mutagenesis in 10-aa windows (highlighted in red) across the entire trans-  
 260 sialidase antigenic fragment demonstrates the seroreactive epitope in Chagas disease.



261 Values are normalized antibody indices and represent the averages of five seropositive  
 262 blood donor specimens.

263 **Evaluation of trans-sialidase antigen TS-2.23 antibody reactivity**

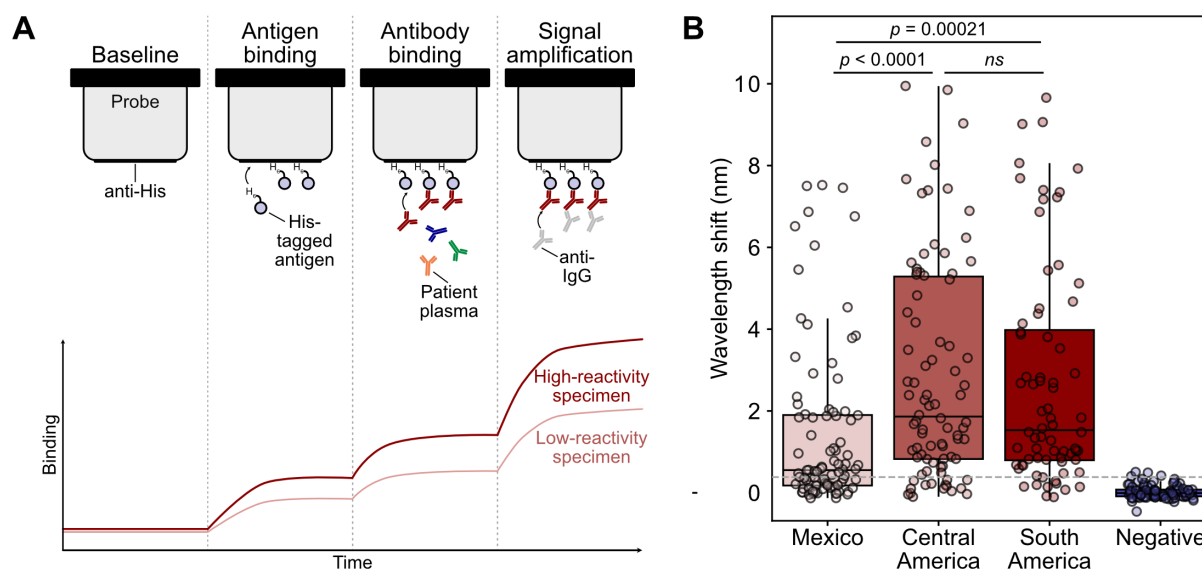
264 To evaluate the potential of TS-2.23 as a diagnostic serology antigen, we compared its PhIP-seq  
 265 performance to that of current diagnostic antigens. To address the fact that current diagnostic  
 266 antigen sequences vary at certain amino acids from available sequencing data (33) and the  
 267 specific antigen sequences used in commercial diagnostics are not publicly available for all  
 268 assay, we agnostically derived the aa sequence motifs of eight diagnostic antigens used in US  
 269 Food and Drug Administration (FDA)-cleared serology tests (24) using Multiple EM for Motif  
 270 Elicitation (MEME) (see *Materials and Methods*) (Fig. S6) (34-36). These motifs were then  
 271 queried against the entire *T. cruzi* PhIP-seq proteome using FIMO to identify all peptides with a  
 272 significantly similar sequence to each antigen (37). The maximum z-score for each BD sample  
 273 across all PhIP-seq peptides with a sequence match to a given antigen motif was plotted (Fig.  
 274 4a). The maximum z-score across all peptides with a sequence match to TS-2.23 was also shown  
 275 to compare the novel antigen reactivity to those in used in current diagnostics. Any sample with  
 276 a z-score of at least 5 for a peptide that contained an antigen motif was considered enriched for  
 277 antibody reactivity prevalence calculations (Fig. 4b). TS-2.23 had high prevalence, demonstrated  
 278 in 100% (64/64) of the seropositive BD samples and 95% (108/114) of CBM seropositive  
 279 samples. By comparison, only Ag 2 and TcE had similar antibody reactivity and prevalence  
 280 across seropositive specimens. In contrast, Ag 1, Ag13 and Ag36 had similar prevalence but  
 281 lower reactivity, and KMP-11 was rarely enriched.  
 282



283  
 284 **Fig. 4. PhIP-seq antibody reactivity of current diagnostic antigens and TS-2.23 within**  
 285 **individual Chagas disease seropositive specimens.** Recombinant antigens in current  
 286 FDA-cleared serology tests include Ag 1, Ag 2, Ag 13, Ag 30, Ag 36 (33, 34), shed acute  
 287 phase antigen (SAPA) (35), KMP-11 (36), TcD and TcE (30, 37). Note, TcD contains the  
 288 same antigenic epitope as Ag 13. (A) Heatmap of z-score enrichment over seronegative  
 289 controls in the seropositive blood donor (BD) specimens (n=64). Each antigen motif was  
 290 derived using Multiple EM for Motif Elicitation (MEME) and then scored against the  
 291 entire *T. cruzi* PhIP-seq proteome. The maximum z-score across all peptides with  
 292 significant sequence matches to a given antigen motif was plotted for each sample and  
 293 each antigen. (B) Percent of samples enriched ( z-score  $\geq 5$ ) for each antigen in BD and  
 294 cardiac biomarker (CBM) specimen sets.

295 To further validate and directly characterize the antibody reactivity of TS-2.23, we performed a  
296 quantitative IgG biolayer interferometry (BLI) immunoassay on 336 BD specimens with  
297 previous Chagas disease serology testing (n=250, seropositive; n=86, seronegative) (*Materials*  
298 *and Methods*, Fig. 5a). Seropositive samples were chosen to include all specimens with region of  
299 origin data (Mexico, n=92; Central America, n=86; South America, n=72) (Fig. 5b). The results  
300 of the pairwise comparisons between regions demonstrated seroreactivity was lower in  
301 individuals from Mexico compared to Central America ( $p < 0.0001$ ) and South America ( $p =$   
302  $0.00021$ ). Specimens from individuals from Central America and South America did not show  
303 differences in reactivity ( $p = 1.000$ ). Seronegative specimens did not demonstrate any overt non-  
304 specific reactivity to the TS-2.23 antigen.

305



306

307 **Fig. 5. Biolayer interferometry validates trans-sialidase antigen TS-2.23 seroreactivity in a**

308 **large cohort.** (A) Schematic of biolayer interferometry (BLI) approach. BLI uses a  
309 fiberoptic probe to measure the wavelength of light reflected from the surface of a  
310 biosensor, which changes due to light interference when an analyte binds. First, an anti-  
311 His tag probe is incubated with His-tagged antigen. Then, the probe is incubated in  
312 diluted serum or plasma, and antibodies bind the immobilized antigen on the probe. To  
313 quantify IgG-specific reactivity, anti-IgG antibodies are added and bind the immobilized  
314 patient antibodies. (B) Seropositive blood donor specimens (n = 250) demonstrate a range  
315 of reactivity to the trans-sialidase antigen by quantitative BLI immunoassay, while  
316 seronegative blood donor specimens (n=86) do not (Wilcoxon rank-sum test). Reactivity,  
317 as denoted by wavelength shift, was higher in Central American (n=86) and South  
318 American (n=72) specimens than in Mexican specimens (n=92). Dashed line  
319 corresponds to the 25th percentile across all seropositive specimens.

320 To evaluate if specimens with low reactivity to TS-2.23 are weakly reactive overall, we  
321 compared TS-2.23 reactivity with previous results from an FDA-cleared Chagas disease serology  
322 ELISA (Chagatest Recombinante v.3.0, Wiener Labs [Wv3]). This assay contains a multi-  
323 epitope recombinant antigen comprised of Ag 1, Ag 2, Ag 13, Ag 30, Ag 36, and SAPA (30, 31).  
324 Analysis of the 25<sup>th</sup> percentile of TS-2.23 BLI reactivity yielded 63 specimens originally positive

325 by blood donor testing. The reactivity (signal-to-cutoff ratio) of the Wv3 ELISA was in the 25<sup>th</sup>  
326 percentile of previous testing (12) for 70% (44/63) of the low reactive TS-2.23 BLI specimens.  
327 This comparison to previous Wv3 ELISA test results suggests that most low reactivity TS-2.23  
328 specimens are weakly reactive specimens overall. Breakdown of these specimens by region of  
329 origin included 60% (38/63) from Mexico, 24% (15/63) from Central America, and 16% (10/63)  
330 from South America.

## 331 **DISCUSSION**

332 Chagas disease is a neglected tropical disease endemic to the Americas, affecting over 6 million  
333 people worldwide (1). Numerous diagnostic challenges for chronic Chagas disease exist,  
334 including low clinical awareness, non-specific or asymptomatic presentation, and imperfect test  
335 performance (38, 39). In addition to better testing for populations with epidemiological risk  
336 factors for exposure to triatomine vectors, effective testing is needed for at-risk people presenting  
337 for prenatal screening, blood donation and organ transplant evaluation (8-11). The major  
338 disparities for Chagas disease serology testing are insufficient sensitivity and specificity of any  
339 one diagnostic test to be used alone and differential serological test performance by region of  
340 origin of *T. cruzi* infection.

341 To address this, we carried out our *T. cruzi* PhIP-seq study in two well-characterized Chagas  
342 disease specimen sets, which represent the largest number of samples evaluated for *T. cruzi*  
343 antigen discovery, to our knowledge. One set (BD) includes specimens from individuals born in  
344 Mexico, Central America and South America, collected via blood donation in the US (12). An  
345 additional set (CBM) includes Bolivians with varying stages of Chagas cardiomyopathy,  
346 collected via a clinical study of cardiac biomarkers (40). Analysis of these two specimen sets by  
347 PhIP-seq identified more than 1,300 reactive *T. cruzi* peptides highly specific to individuals with  
348 Chagas disease. Down selection on common antigens amongst Chagas disease seropositive  
349 individuals filtered to only three antigenic sequences with sufficient prevalence for diagnostic  
350 utility (enrichment in  $\geq 90\%$  of specimens). This vast difference between total reactive peptides  
351 and high-prevalence antigens illustrates the uniqueness of the adaptive immune system response  
352 within an individual host. By contrast, the rare high-prevalence antigens warrant further research  
353 into the host-pathogen biology that drives their immunodominance.

354 Two of these high-prevalence antigens were identified by multiple groups from early phage  
355 display studies and are already incorporated into current serological diagnostics: Ag 2 (30, 31), a  
356 nucleoporin protein, and TcE (41), a 60S ribosomal subunit protein. The third and, in fact, most  
357 prevalent peptide antigen discovered in our study, TS-2.23, has not previously been described as  
358 a serological diagnostic antigen and belongs to the trans-sialidase family. Trans-sialidase  
359 enzymes comprise a unique pathogenic and antigenic family of secreted and  
360 glycosylphosphatidylinositol (GPI)-anchored cell surface proteins in *T. cruzi*. Their primary  
361 functional activity is to transfer sialic acids from mammalian cells to beta-galactosidase residues  
362 on *T. cruzi*'s cell membrane to assist in cell invasion (42). Trans-sialidases also appear to  
363 modulate the host immune response, likely acting as decoy antigens (43). The evidence for this  
364 relates to the discovery of the shed acute phase antigen (SAPA), a multi-repeat antigen located at  
365 the C-terminal end of trans-sialidase enzymes (44). Since the catalytic end is in the N-terminal  
366 region, it is hypothesized that C-terminal antigens evolved to protect the trans-sialidase enzyme  
367 activity from humoral responses. BLAST analysis of the trans-sialidase antigen identified by our  
368 study showed 37 *T. cruzi* proteins with  $>93\%$  sequence identity, all of which were trans-sialidase

369 or putative trans-sialidase genes. All sequences were located at C-terminal end, matching with  
370 the immunodominant nature of known antigens from this family.

371 Our findings also demonstrate that the TS-2.23 antigen identified in this study has increased  
372 antibody reactivity in specimens from individuals born in Central America, compared to  
373 previous analyses of the same specimens by current clinical diagnostics (12). Beyond the  
374 potential implications for endemic populations in Central America, identification of TS-2.23 is  
375 important for screening and diagnosis in the US considering that a large proportion of the Latin  
376 American immigrant population is predominantly from El Salvador and Guatemala. Further  
377 studies evaluating Central American Chagas disease populations with a combination of  
378 conventional antigens and TS-2.23 will be needed to identify real-world increases in diagnostic  
379 test performance. While this is a promising advancement, unfortunately, TS-2.23 does not have  
380 improved seroreactivity in individuals who acquired *T. cruzi* infection in Mexico. Further study  
381 is needed to evaluate whether this is due to lower anti-*T. cruzi* IgG levels in individuals exposed  
382 in Mexico or the absence of regional *T. cruzi* antigens of Mexican origin. Post-translational  
383 protein glycosylation may be a source of unique antigenicity outside of the primary peptide  
384 sequence (45).

385 Our study is limited by retrospective selection bias on samples tested by current diagnostic  
386 assays. Prospective testing in at-risk populations will be important to further validate the TS-2.23  
387 antigen. We do not report on the sensitivity or specificity of the TS-2.23 antigen in comparison  
388 to previous testing because these assays contain between 6 to 9 different antigens in a  
389 multiepitope format. The evaluation of test performance by TS-2.23 should be done in  
390 combination with these recombinant multiepitope assays to generate test performance  
391 characteristics, which are planned for follow-on studies. Ultimately, to create the ideal serologic  
392 test for diagnosis of chronic Chagas disease, we would combine the fewest recombinant targets  
393 for a multiepitope antigen that approaches 100% sensitivity and specificity to eliminate the need  
394 for confirmatory testing for all initial *T. cruzi* seropositive results. Such a test would greatly  
395 facilitate Chagas disease screening, diagnosis, and treatment.

396 In summary, our study has discovered a novel *T. cruzi* trans-sialidase peptide antigen (TS-2.23)  
397 that is serologically reactive and prevalent across endemic countries of Latin America and  
398 varying degrees of cardiac disease severity. Future studies will evaluate the real-world test  
399 performance in traditional immunoassay formats common in clinical laboratories.

## 400 MATERIALS AND METHODS

### 401 Study Design

402 Samples used in this study included blood donor plasma collected within the US and serum from  
403 clinical research collected in Bolivia. The blood donor plasma samples were provided in  
404 collaboration with the American Red Cross (ARC) with sample selection criteria described  
405 previously (12). All blood donor specimens (BD) were confirmed by blood donor testing assays  
406 and algorithms (9). A subset of specimens was used for antigen discovery experiments (n=90;  
407 n=64, seropositive; n=26, seronegative). Region of origin data was available for 35 specimens  
408 (n=13, Mexico; n=10, Central America; n=12, South America). The serum samples from clinical  
409 research studies in Bolivia were collected as part of a cardiac biomarker (CBM) study (40).  
410 Specimens were collected from a large public hospital in Santa Cruz, tested and confirmed for *T.*  
411 *cruzi* serostatus and further stratified for cardiac status by clinical assessment, electrocardiogram  
412 and echocardiography studies. In total, 143 serum samples were included for this study,

413 including 22 seronegative (n=15, without significant cardiac abnormalities [Stage A]; n=7, with  
414 cardiac abnormalities [Stage B]) and 121 seropositive (n=40, without significant cardiac  
415 abnormalities [Stage A]; n= 81, with cardiac abnormalities[Stages B-D]). Cardiac staging is  
416 defined as: A, normal electrocardiogram (ECG), normal echocardiography (echo); B, abnormal  
417 ECG, normal echo; C, 40-55% ejection fraction (EF) by echo, normal left ventricular end  
418 diastolic diameter (LVEDD); D, EF<40% or LVEDD >57mm. Specimens were randomized to  
419 96-well plates prior to testing and frozen at -20°C. A separate set of *T. cruzi* seronegative plasma  
420 specimens (n=95) from the New York Blood Center (NYBC) was used as an independent  
421 negative control for antigen discovery experiments with the CBM specimen set.

422 Institutional review board for research use of de-identified human biospecimens was approved  
423 by the University of California San Francisco. The BD study protocol was approved by  
424 institutional review board at the American Red Cross. The CBM study protocol was approved by  
425 the Institutional Review Boards of Universidad Catolica Boliviana (Santa Cruz, Bolivia) and  
426 included consent for future use of deidentified specimens (40). NYBC specimens consisted of  
427 de-identified plasma obtained from adults who donated blood to the New York Blood Center.

#### 428 **Construction of *T. cruzi* phage library**

429 Reference protein sequences for the *T. cruzi* strain CL Brener assembly GCF\_000209065.1 (46)  
430 were obtained from the National Center of Biotechnology Information (NCBI) site. All  
431 sequences in the peptidome were processed using a previously described bioinformatic pipeline  
432 (47). Briefly, all full-length protein sequences were decomposed into a series of overlapping  
433 peptides. Each peptide was 47 amino acids in length with consecutive peptides overlapping by  
434 19 amino acids. The full set of peptides was collapsed using the command line tool cd-hit (48,  
435 49) at 90% sequence similarity, resulting in a final set of 228,127 peptides spanning the *T. cruzi*  
436 peptidome (19,607 proteins). Peptides tiling over the length of the glial fibrillary acidic protein  
437 (GFAP) were added to the library as a positive control for immunoprecipitation. Peptide  
438 sequences were converted to their coding DNA sequences with common 5'  
439 (GTAGCTGGTGTGTAGCTGCC) and 3' (GGTGACTACAAGGATGATGATGATAAA)  
440 linker sequences appended to each peptide encoding sequence. The 3' linker sequence encoded a  
441 FLAG tag). The final library, consisting of 228,162 peptides that correspond to 19,608 proteins,  
442 was ordered from Agilent Technologies.

#### 443 **Cloning and packaging into T7 phage**

444 The oligo pool was received in a single tube, lyophilized, and was resuspended to 0.2 nM. The  
445 pool was amplified using Phusion polymerase (New England Biolabs [NEB]) and linker-specific  
446 primers (TAGTTAAGCGGAATTCAGTAGCTGGTGTGTAGCTGCC,  
447 ATCCTGAGCTAAGCTTTTATCATCATCATCCTTGTAGTCACC). The amplified library  
448 was purified using Ampure XP magnetic beads (Beckman Coulter) and confirmed to have a  
449 single-size product by gel electrophoresis. One µg of the cleaned library was then digested using  
450 EcoRI-HF and HindIII-HF restriction enzymes (NEB) and purified again using Ampure XP  
451 beads. Digestion of the library product was confirmed by visualizing a 20bp size shift using the  
452 Bioanalyzer High Sensitivity DNA Analysis kit (Agilent). The digested library was cloned into  
453 T7 Select vector arms (Novagen 70550-3) as previously described (47). Four packaging  
454 reactions were performed and then pooled. The final phage library was grown up in BLT5403 *E.*  
455 *coli* (Novagen 70550-3).

#### 456 **Immunoprecipitation of antibody-bound phage**

457 PhIP-seq was performed using the *T. cruzi* peptide phage display library with plasma or serum  
458 samples using our previously-published PhIP-seq protocol ([https://www.protocols.io/view/derisi-  
459 lab-phage-immunoprecipitation-sequencing-ph-4r3l229qx11y/v1](https://www.protocols.io/view/derisi-lab-phage-immunoprecipitation-sequencing-ph-4r3l229qx11y/v1)). Patient plasma was diluted 1:1  
460 in storage buffer (0.04% NaN<sub>3</sub>, 40% Glycerol, 40 mM HEPES (pH 7.3), 1 x PBS (-Ca and -  
461 Mg)) to preserve antibody integrity. One uL of diluted plasma was incubated with 500 μL of the  
462 input phage display library for the first round of immunoprecipitation. Positive control  
463 immunoprecipitations were performed using 1 μL of 1:10 diluted anti-GFAP antibody (Dako,  
464 Z0334) (Figure S2). Ten μL of Dynabeads Protein A/G slurry (ThermoFisher Scientific) were  
465 used per sample. After one round of immunoprecipitation, phage were amplified in *E. coli* and  
466 enriched in a second round of immunoprecipitation. The final lysate was spun and stored at 4 °C  
467 for NGS library prep. Immunoprecipitated phage lysate was heated to 70 °C for 15 min to expose  
468 DNA. DNA was then prepared for next-generation sequencing in two subsequent PCR  
469 amplifications. The final prepared libraries were sequenced using an Illumina sequencer to a read  
470 depth of approximately 1 million reads per sample.

### 471 **PhIP-seq data analysis**

472 Sequencing reads from fastq files were aligned to the reference *T. cruzi* peptide library and  
473 individual peptide counts were normalized to reads per 100,000 (RPK) by dividing by the sum of  
474 counts and multiplying by 100,000 to account for varying read depth. All subsequent analyses  
475 were performed using Python (version 3.12.2) unless otherwise noted.

476 To identify Chagas disease-specific enriched peptides and avoid false positives, a conservative  
477 analysis pipeline was used as follows. Peptide-level enrichment across known seronegative  
478 samples was calculated and used to generate z-scores ((x-mean seronegative)/standard deviation  
479 seronegative) for the Chagas disease seropositive, seronegative, and NYBC control samples. The  
480 z-score for any seronegative sample was calculated by leaving out that sample from the mean of  
481 seronegative samples for each peptide. A moving threshold analysis was implemented to  
482 determine the z-score threshold and the number of Chagas disease patients that must share  
483 enrichment to a given peptide to completely differentiate seropositive and seronegative patients  
484 (Figure S3). Based on this analysis, z-score cutoff of 5 and shared enrichment across at least five  
485 percent of Chagas disease samples ( $n \geq 3$  BD specimens;  $n \geq 5$  CBM specimens) and one or fewer  
486 seronegative samples was set for hit calling.

487 Additional validation of the z-score approach was executed using a mass univariate analysis  
488 using generalized linear models applied to each peptide. Peptide fragments with uniform values  
489 across all samples were removed due to lack of variability. RPK values were scaled by  
490 subtracting the mean and dividing by the standard deviation calculated within each peptide.  
491 Scaled RPK values for each peptide were regressed on Chagas disease diagnostic status ( $y_i = \beta_{0i}$   
492  $+ \beta_{1i} \cdot x$ ) where  $y_i$  is the scaled RPK value,  $\beta_{0i}$  is the intercept of the  $i$ -th peptide fragment,  $\beta_{1i}$  is  
493 the predictor coefficient, and  $x$  is the diagnostic status in BD samples or cardiac disease stage in  
494 CBM samples. The resulting coefficient quantified the strength and direction of the association  
495 between diagnostic status (or disease stage) and the scaled RPK values for each peptide, where  
496 positive coefficient values represent, on average, a higher RPK for that peptide in seropositive  
497 specimens. Analyses were performed using R (version 4.3.1).

498 Antigenic prevalence of a *T. cruzi* peptide was calculated as the number of seropositive samples  
499 enriched for a specific peptide divided by the number of seropositive samples in the respective

500 specimen set (BD and CBM). High-prevalence antigens were designated as enrichment in  $\geq 90\%$   
501 of seropositive specimens and no seronegative specimens.

### 502 **Split Luciferase Binding Assay (SLBA)**

503 A high-prevalence antigen by PhIP-seq that was not already included in commercial diagnostics  
504 was selected for orthogonal validation by SLBA. A detailed SLBA protocol can be found online  
505 at <https://www.protocols.io/view/split-luciferase-binding-assay-slba-protocol-4r3l27b9pg1y/v1>.  
506 Briefly, the high-prevalence peptide antigen was inserted into a split luciferase construct  
507 containing a T7 promoter and a terminal HiBiT tag and synthesized as DNA oligomers (Twist  
508 Biosciences). The oligos were amplified using 5'-  
509 AAGCAGAGCTCGTTTAGTGAACCGTCAGA-3' and 5'-  
510 GGCCGGCCGTTTAAACGCTGATCTT-3' primer pair and purified using the DNA Clean and  
511 Concentrator-5 kit (Zymo). Purified PCR products were transcribed and translated *in vitro*  
512 (IVTT) using wheat germ extract (Promega L4140) and the Nano-Glo HiBiT Lytic Detection  
513 System (Promega, N3040) was used to quantify translated protein using relative luciferase units  
514 (RLU) detected on a luminometer. Background luminescence was calculated using an IVTT  
515 reaction that used a construct encoding a STOP codon 5' of the HiBiT tag. Peptides were  
516 normalized to  $2 \times 10^7$  RLU per well, incubated overnight with patient plasma or a positive  
517 control anti-HiBiT antibody (Promega, N7200), and immunoprecipitated with a Dynabeads  
518 Protein A/G bead slurry. The immunoprecipitation was washed four times with SLBA buffer  
519 (0.15 M NaCl, 0.02 M Tris-HCl pH 7.4, 1% w/v sodium azide, 1% w/v bovine serum albumin,  
520 and 0.15% v/v Tween 20) and remaining luminescence was measured using the Nano-Glo HiBiT  
521 Lytic Detection System in a luminometer. Antibody index was calculated as (RLU sample –  
522 RLU mock IP)/(RLU sample – RLU anti-HiBiT) for orthogonal validation of the trans-sialidase  
523 peptides. For epitope mapping by alanine-scanning mutagenesis, the antibody index was  
524 calculated as (RLU seropositive – RLU US control)/(RLU seropositive – RLU anti-HiBiT) and  
525 normalized to the antibody index of immunoprecipitation using the wild-type peptide sequence.

### 526 **MEME and FIMO Motif Analysis**

527 To empirically re-derive a selected diagnostic antigen motif, all BD-enriched peptides were  
528 filtered to those peptides that mapped to the antigenic protein (e.g., any enriched peptide that  
529 belonged to a nucleoporin protein for Ag2). These peptide sequences were queried using *MEME*  
530 (*MEME* 5.5.7) with the following *meme* command options and parameters:

531 `-protein -mod zoops -nmotifs 10 -minw 6 -maxw 15 -objfun classic -markov_order 0`

532 The derived motifs were then manually inspected to identify the motif that clearly matched the  
533 published diagnostic antigen sequences (Figure S6) (24). This motif (or multiple motifs, if the  
534 antigen sequence was over 47 amino acids, as in the case of Ag1 and Ag36) was then queried  
535 against the entire *T. cruzi* PhIP-seq proteome using the following *fimo* command options and  
536 parameters:

537 `--thresh 1e-4 --qv-thresh`

538 The only exceptions to this analysis were antigens Ag13, TcE, and KMP-11. Ag13 and TcE are  
539 short, highly repetitive antigens, and so were identified using the *meme* parameter -mod anr. The  
540 final antigenic motif identified for TcE was very short (6 amino acids) and thus required  
541 different *fimo* significance thresholds to identify similar sequences. A q-value threshold of  $1e-2$   
542 was set for this antigen only. Finally, KMP-11 was represented by only three overlapping

543 peptides that map to kinetoplastid membrane protein KMP-11 (XP\_808865.1), so motif  
544 discovery was not possible. To look for sequence similarity across the *T. cruzi* proteome, the 92-  
545 amino acid KMP-11 protein was queried against the proteome using *blastp* (BLAST 2.12.0) and  
546 no other peptides with significant sequence similarity were identified. The three KMP-11  
547 peptides alone were used for downstream analysis of KMP-11 antigen reactivity.

548 To assess the reactivity of patient samples against these antigen motifs, the maximum z-score  
549 across all peptides with a sequence match to a given antigen motif was plotted for each BD  
550 sample.

### 551 **Peptide Antigen Expression**

552 We selected a minimal antigenic peptide sequence that consisted of the 15-aa that, when mutated  
553 via alanine scanning, produced the lowest binding signal on SLBA (Figure 3c), to test using  
554 biolayer interferometry (BLI). This peptide sequence was repeated seven times in series to create  
555 a final protein that was approximately 13 kDa. The insert sequence was synthesized by Twist  
556 Bioscience in a pET-21(+) vector, with a C-terminal 6X His tag and under control of a T7  
557 promoter and lac repressor.

558 The expression plasmid was transformed into BL21(DE3) competent *E. coli* (Thermo  
559 Scientific) and plated onto Luria-Bertani (LB) agar plates containing carbenicillin. Isolates were  
560 expanded in 1L LB broth with carbenicillin grown at 37°C to an OD600 of 0.6. The culture was  
561 induced with 1mM Isopropyl  $\beta$ -D-1-thiogalactopyranoside and grown at 25°C shaking for  
562 another 18 hours. The cells were then centrifuged at 10,000 RPM for 30 minutes at 4°C to collect  
563 the cell pellet.

564 A stock lysis buffer (20 mM sodium phosphate, 20 mM imidazole, 500 mM NaCl, 0.5 mM  
565 TCEP, 5% glycerol, pH 7.4) was made with EDTA-free (Roche) per 50 mL. The pelleted cells  
566 were resuspended in 100mL of cold lysis buffer and run through a LM10 microfluidizer at  
567 15,000 PSI for 5 cycles. The flowthrough lysate was collected after each cycle and combined.  
568 The lysate was centrifuged at 12,500 RPM for 30 minutes at 4°C. The supernatant was collected  
569 and filtered through a 0.22  $\mu$ m vacuum filtration device.

570 Recombinant His-tagged antigen was purified from the filtered lysate using a Ni-NTA resin  
571 gravity flow column. After loading the lysate to the column, the column was washed with a wash  
572 buffer (20 mM sodium phosphate, 40 mM imidazole, 500 mM NaCl, 0.5 mM TCEP, pH 7.4).  
573 The antigen was eluted with an elution buffer (20 mM sodium phosphate, 500 mM imidazole,  
574 500 mM NaCl, 0.5 mM TCEP, pH 7.4). Peptide yield from the purification was quantified using  
575 NanoDrop (Thermo Scientific), and the purity of the product was verified by protein gel  
576 electrophoresis. Expression of the peptide was confirmed by anti-His tag Western blot using a  
577 6X-His tag monoclonal antibody (Invitrogen, MA1-21315).

### 578 **Biolayer Interferometry (BLI) Serological Immunoassay**

579 A GatorPrime analyzer (Gator Bio) was used to perform BLI to evaluate the antibody reactivity  
580 to the recombinant peptide antigen. BLI uses a fiberoptic probe to measure the wavelength of  
581 light (nanometers [nm]) reflected from the surface of a biosensor, which shifts in response to  
582 analyte binding (Figure 5a). Quantitative BLI serological immunoassay can be performed by  
583 measuring nm shift to antigen-bound probe incubated in diluted serum or plasma and  
584 subsequently in anti-human immunoglobulin (IgG) for quantifying class-specific responses. BLI  
585 methodology was chosen for these analyses because it has a higher dynamic range for assessing



586 antibody-antigen reactivity compared to traditional colorimetric enzyme-linked immunosorbent  
587 assays (ELISA) (50). An anti-*T. cruzi* IgG BLI method was developed using a commercial *T.*  
588 *cruzi* Chimeric Chagas Multi-Antigen (MACH; Jena Biosciences). This is a polypeptide chain of  
589 87-aas with epitopes from previously known antigens: Peptide 2, TcD, TcE, and SAPA, fused  
590 with a 6His-Tag. This BLI method was optimized using high, intermediate, and low reactivity  
591 seropositive BD specimens previously determined by Chagatest Recombinante v.3.0 anti-*T.cruzi*  
592 ELISA (Wiener Labs), which contain the MACH antigens.

593 The anti-*T.cruzi* IgG BLI assay was adapted for the recombinant antigen discovered by PhIP-seq  
594 by varying the protein concentration to achieve saturation of nm shift signal of the anti-His tag  
595 fiberoptic probe (Figure S7). The final method consisted of the following BLI conditions: 1) 600  
596 second (s) incubation of anti-His probe in 2ug/mL peptide antigen, 2) 1800s incubation in 10uL  
597 of plasma diluted 1:19 with Q-Buffer diluent (GatorBio), and 3) 2000s incubation in a solution of  
598 10ug/mL goat anti-human IgG (Jackson ImmunoResearch). Steps 1 and 2 were followed by a  
599 360s wash in Q-Buffer. Endpoint nm shift measurements were normalized by subtracting the nm  
600 shift value after antigen loading wash (step 1) to account for any minor variation in the amount  
601 of immobilized antigen.

602 Anti-*T. cruzi* IgG BLI was performed on 336 BD specimens (n = 250, seropositive; n=86,  
603 seronegative) to evaluate antibody reactivity to the peptide antigen. Region of origin data was  
604 available for all seropositive specimens (Mexico, n=92; Central America, n=86; South America,  
605 n=72). Wilcoxon rank sum analysis with a correction for multiple comparisons using the  
606 Bonferroni method was completed to compare reactivity between regions.

## 607 **Statistical analysis**

608 Associations between number of individual antibody targets and heart disease stage or region of  
609 infection were tested using Kruskal-Wallis tests. Motif analysis was performed using MEME and  
610 FIMO (34-36). Associations between anti-TS-2.23 BLI reactivity, serologic status, and region  
611 were tested using the Wilcoxon rank-sum test with a correction for multiple comparisons using  
612 the Bonferroni method.

613

## 614 **List of Supplementary Materials**

615 Fig. S1 to S7

616 Table S1

617

## 618 **References and Notes**

- 619 1. S. World Health Organization = Organisation mondiale de la, Chagas disease in Latin  
620 America : an epidemiological update based on 2010 estimates = Maladie de Chagas en  
621 Amérique latine : le point épidémiologique basé sur les estimations de 2010. *Weekly*  
622 *Epidemiological Record = Relevé épidémiologique hebdomadaire* **90**, 33-44 (2015).
- 623 2. A. Irish, J. D. Whitman, E. H. Clark, R. Marcus, C. Bern, Updated Estimates and  
624 Mapping for Prevalence of Chagas Disease among Adults, United States. *Emerg Infect*  
625 *Dis* **28**, 1313-1320 (2022).
- 626 3. C. Bern, L. A. Messenger, J. D. Whitman, J. H. Maguire, Chagas Disease in the United  
627 States: a Public Health Approach. *Clin Microbiol Rev* **33**, (2019).

- 628 4. M. C. P. Nunes, A. Beaton, H. Acquatella, C. Bern, A. F. Bolger, L. E. Echeverria, W. O.  
629 Dutra, J. Gascon, C. A. Morillo, J. Oliveira-Filho, A. L. P. Ribeiro, J. A. Marin-Neto, E.  
630 American Heart Association Rheumatic Fever, Y. Kawasaki Disease Committee of the  
631 Council on Cardiovascular Disease in the, C. Council on, N. Stroke, C. Stroke, Chagas  
632 Cardiomyopathy: An Update of Current Clinical Knowledge and Management: A  
633 Scientific Statement From the American Heart Association. *Circulation* **138**, e169-e209  
634 (2018).
- 635 5. A. Perez-Ayala, J. A. Perez-Molina, F. Norman, B. Monge-Maillo, M. V. Faro, R. Lopez-  
636 Velez, Gastro-intestinal Chagas disease in migrants to Spain: prevalence and methods for  
637 early diagnosis. *Ann Trop Med Parasitol* **105**, 25-29 (2011).
- 638 6. R. B. de Oliveira, L. E. Troncon, R. O. Dantas, U. G. Menghelli, Gastrointestinal  
639 manifestations of Chagas' disease. *Am J Gastroenterol* **93**, 884-889 (1998).
- 640 7. Pan American Health Organization. (2019), vol. 2021.
- 641 8. C. J. Forsyth, J. Manne-Goehler, C. Bern, J. Whitman, N. S. Hochberg, M. Edwards, R.  
642 Marcus, N. L. Beatty, Y. E. Castro-Sesquen, C. Coyle, P. Stigler Granados, D. Hamer, J.  
643 H. Maguire, R. H. Gilman, S. Meymandi, Recommendations for Screening and Diagnosis  
644 of Chagas Disease in the United States. *J Infect Dis* **225**, 1601-1610 (2022).
- 645 9. R. Y. Dodd, J. A. Groves, R. L. Townsend, E. P. Notari, G. A. Foster, B. Custer, M. P.  
646 Busch, S. L. Stramer, Impact of one-time testing for *Trypanosoma cruzi* antibodies  
647 among blood donors in the United States. *Transfusion* **59**, 1016-1023 (2019).
- 648 10. O. P. T. N. . (2023), vol. 2023.
- 649 11. P. V. Chin-Hong, B. S. Schwartz, C. Bern, S. P. Montgomery, S. Kontak, B. Kubak, M. I.  
650 Morris, M. Nowicki, C. Wright, M. G. Ison, Screening and treatment of chagas disease in  
651 organ transplant recipients in the United States: recommendations from the chagas in  
652 transplant working group. *Am J Transplant* **11**, 672-680 (2011).
- 653 12. J. D. Whitman, C. A. Bulman, E. L. Gunderson, A. M. Irish, R. L. Townsend, S. L.  
654 Stramer, J. A. Sakanari, C. Bern, Chagas Disease Serological Test Performance in U.S.  
655 Blood Donor Specimens. *J Clin Microbiol* **57**, (2019).
- 656 13. Y. E. Castro-Sesquen, A. Saldana, D. Patino Nava, T. Bayangos, D. Paulette Evans, K.  
657 DeToy, A. Trevino, R. Marcus, C. Bern, R. H. Gilman, K. R. Talaat, P. Chagas Working  
658 Group in, S. the United, Use of a Latent Class Analysis in the Diagnosis of Chronic  
659 Chagas Disease in the Washington Metropolitan Area. *Clin Infect Dis* **72**, e303-e310  
660 (2021).
- 661 14. C. Truyens, E. Dumonteil, J. Alger, M. L. Cafferata, A. Ciganda, L. Gibbons, C. Herrera,  
662 S. Sosa-Estani, P. Buekens, Geographic Variations in Test Reactivity for the Serological  
663 Diagnosis of *Trypanosoma cruzi* Infection. *J Clin Microbiol* **59**, e0106221 (2021).
- 664 15. E. A. Kelly, C. A. Bulman, E. L. Gunderson, A. M. Irish, R. L. Townsend, J. A. Sakanari,  
665 S. L. Stramer, C. Bern, J. D. Whitman, Comparative Performance of Latest-Generation  
666 and FDA-Cleared Serology Tests for the Diagnosis of Chagas Disease. *J Clin Microbiol*,  
667 (2021).
- 668 16. J. R. Verani, A. Seitz, R. H. Gilman, C. LaFuente, G. Galdos-Cardenas, V. Kawai, E. de  
669 LaFuente, L. Ferrufino, N. M. Bowman, V. Pinedo-Cancino, M. Z. Levy, F. Steurer, C.  
670 W. Todd, L. V. Kirchhoff, L. Cabrera, M. Verastegui, C. Bern, Geographic variation in  
671 the sensitivity of recombinant antigen-based rapid tests for chronic *Trypanosoma cruzi*  
672 infection. *Am J Trop Med Hyg* **80**, 410-415 (2009).

- 673 17. D. Guzman-Gomez, A. Lopez-Monteon, M. de la Soledad Lagunes-Castro, C. Alvarez-  
674 Martinez, M. J. Hernandez-Lutzon, E. Dumonteil, A. Ramos-Ligonio, Highly discordant  
675 serology against *Trypanosoma cruzi* in central Veracruz, Mexico: role of the antigen used  
676 for diagnostic. *Parasit Vectors* **8**, 466 (2015).
- 677 18. E. Z. Caballero, R. Correa, M. S. Nascimento, A. Villarreal, A. Llanes, N. Kesper, Jr.,  
678 High sensitivity and reproducibility of in-house ELISAs using different genotypes of  
679 *Trypanosoma cruzi*. *Parasite Immunol* **41**, e12627 (2019).
- 680 19. R. Gamboa-Leon, C. Gonzalez-Ramirez, N. Padilla-Raygoza, S. Sosa-Estani, A. Caamal-  
681 Kantun, P. Buekens, E. Dumonteil, Do commercial serologic tests for *Trypanosoma cruzi*  
682 infection detect Mexican strains in women and newborns? *J Parasitol* **97**, 338-343  
683 (2011).
- 684 20. B. Zingales, M. A. Miles, D. A. Campbell, M. Tibayrenc, A. M. Macedo, M. M. Teixeira,  
685 A. G. Schijman, M. S. Llewellyn, E. Lages-Silva, C. R. Machado, S. G. Andrade, N. R.  
686 Sturm, The revised *Trypanosoma cruzi* subspecific nomenclature: rationale,  
687 epidemiological relevance and research applications. *Infect Genet Evol* **12**, 240-253  
688 (2012).
- 689 21. A. Marcili, L. Lima, M. Cavazzana, A. C. Junqueira, H. H. Veludo, F. Maia Da Silva, M.  
690 Campaner, F. Paiva, V. L. Nunes, M. M. Teixeira, A new genotype of *Trypanosoma*  
691 *cruzi* associated with bats evidenced by phylogenetic analyses using SSU rDNA,  
692 cytochrome b and Histone H2B genes and genotyping based on ITS1 rDNA.  
693 *Parasitology* **136**, 641-655 (2009).
- 694 22. K. A. Alroy, C. Huang, R. H. Gilman, V. R. Quispe-Machaca, M. A. Marks, J. Ancca-  
695 Juarez, M. Hillyard, M. Verastegui, G. Sanchez, L. Cabrera, E. Vidal, E. M. Billig, V. A.  
696 Cama, C. Naquira, C. Bern, M. Z. Levy, P. Working Group on Chagas Disease in,  
697 Prevalence and Transmission of *Trypanosoma cruzi* in People of Rural Communities of  
698 the High Jungle of Northern Peru. *PLoS Negl Trop Dis* **9**, e0003779 (2015).
- 699 23. J. D. Ramirez, C. Hernandez, *Trypanosoma cruzi* I: Towards the need of genetic  
700 subdivision?, Part II. *Acta Trop* **184**, 53-58 (2018).
- 701 24. T. Bhattacharyya, N. Murphy, M. A. Miles, Diversity of Chagas disease diagnostic  
702 antigens: Successes and limitations. *PLOS Neglected Tropical Diseases* **18**, e0012512  
703 (2024).
- 704 25. G. Cooley, R. D. Etheridge, C. Boehlke, B. Bundy, D. B. Weatherly, T. Minning, M.  
705 Haney, M. Postan, S. Laucella, R. L. Tarleton, High throughput selection of effective  
706 serodiagnostics for *Trypanosoma cruzi* infection. *PLoS Negl Trop Dis* **2**, e316 (2008).
- 707 26. A. D. Ricci, L. Bracco, E. Salas-Sarduy, J. M. Ramsey, M. S. Nolan, M. K. Lynn, J.  
708 Altcheh, G. E. Ballering, F. Torrico, N. Kesper, J. C. Villar, I. S. Marcipar, J. D. Marco,  
709 F. Aguero, The *Trypanosoma cruzi* Antigen and Epitope Atlas: antibody specificities in  
710 Chagas disease patients across the Americas. *Nat Commun* **14**, 1850 (2023).
- 711 27. A. Majeau, E. Dumonteil, C. Herrera, Identification of highly conserved *Trypanosoma*  
712 *cruzi* antigens for the development of a universal serological diagnostic assay. *Emerg*  
713 *Microbes Infect* **13**, 2315964 (2024).
- 714 28. D. Mohan, D. L. Wansley, B. M. Sie, M. S. Noon, A. N. Baer, U. Laserson, H. B.  
715 Larman, PhIP-Seq characterization of serum antibodies using oligonucleotide-encoded  
716 peptidomes. *Nat Protoc* **13**, 1958-1978 (2018).

- 717 29. J. A. Atwood, 3rd, D. B. Weatherly, T. A. Minning, B. Bundy, C. Cavola, F. R.  
718 Opperdoes, R. Orlando, R. L. Tarleton, The Trypanosoma cruzi proteome. *Science* **309**,  
719 473-476 (2005).
- 720 30. C. F. Ibanez, J. L. Affranchino, A. C. Frasch, Antigenic determinants of Trypanosoma  
721 cruzi defined by cloning of parasite DNA. *Mol Biochem Parasitol* **25**, 175-184 (1987).
- 722 31. C. F. Ibanez, J. L. Affranchino, R. A. Macina, M. B. Reyes, S. Leguizamon, M. E.  
723 Camargo, L. Aslund, U. Pettersson, A. C. Frasch, Multiple Trypanosoma cruzi antigens  
724 containing tandemly repeated amino acid sequence motifs. *Mol Biochem Parasitol* **30**,  
725 27-33 (1988).
- 726 32. R. L. Houghton, D. R. Benson, L. D. Reynolds, P. D. McNeill, P. R. Sleath, M. J. Lodes,  
727 Y. A. Skeiky, D. A. Leiby, R. Badaro, S. G. Reed, A multi-epitope synthetic peptide and  
728 recombinant protein for the detection of antibodies to Trypanosoma cruzi in  
729 radioimmunoprecipitation-confirmed and consensus-positive sera. *J Infect Dis* **179**, 1226-  
730 1234 (1999).
- 731 33. A. Majeau, L. Murphy, C. Herrera, E. Dumonteil, Assessing Trypanosoma cruzi Parasite  
732 Diversity through Comparative Genomics: Implications for Disease Epidemiology and  
733 Diagnostics. *Pathogens* **10**, (2021).
- 734 34. R. L. Houghton, Y. Y. Stevens, K. Hjerrild, J. Guderian, M. Okamoto, M. Kabir, S. G.  
735 Reed, D. A. Leiby, W. J. Morrow, M. Lorca, S. Raychaudhuri, Lateral flow immunoassay  
736 for diagnosis of Trypanosoma cruzi infection with high correlation to the  
737 radioimmunoprecipitation assay. *Clin Vaccine Immunol* **16**, 515-520 (2009).
- 738 35. Wiener Lab Group. (2004), vol. 2020.
- 739 36. T. L. Bailey, C. Elkan, Fitting a mixture model by expectation maximization to discover  
740 motifs in biopolymers. *Proc Int Conf Intell Syst Mol Biol* **2**, 28-36 (1994).
- 741 37. C. E. Grant, T. L. Bailey, W. S. Noble, FIMO: scanning for occurrences of a given motif.  
742 *Bioinformatics* **27**, 1017-1018 (2011).
- 743 38. K. K. Stimpert, S. P. Montgomery, Physician awareness of Chagas disease, USA. *Emerg*  
744 *Infect Dis* **16**, 871-872 (2010).
- 745 39. E. A. Kelly, J. I. Echeverri Alegre, K. Promer, J. Hayon, R. Iordanov, K. Rangwalla, J. J.  
746 Zhang, Z. Fang, C. Huang, C. E. Bittencourt, S. Reed, R. M. Andrade, C. Bern, E. H.  
747 Clark, J. D. Whitman, Chagas Disease Diagnostic Practices at Four Major Hospital  
748 Systems in California and Texas. *J Infect Dis* **229**, 198-202 (2024).
- 749 40. E. E. Okamoto, J. E. Sherbuk, E. H. Clark, M. A. Marks, O. Gandarilla, G. Galdos-  
750 Cardenas, A. Vasquez-Villar, J. Choi, T. C. Crawford, R. Q. Do, A. B. Fernandez, R.  
751 Colanzi, J. L. Flores-Franco, R. H. Gilman, C. Bern, B. Chagas Disease Working Group  
752 in, Peru, Biomarkers in Trypanosoma cruzi-infected and uninfected individuals with  
753 varying severity of cardiomyopathy in Santa Cruz, Bolivia. *PLoS Negl Trop Dis* **8**, e3227  
754 (2014).
- 755 41. D. F. Hoft, K. S. Kim, K. Otsu, D. R. Moser, W. J. Yost, J. H. Blumin, J. E. Donelson, L.  
756 V. Kirchhoff, Trypanosoma cruzi expresses diverse repetitive protein antigens. *Infect*  
757 *Immun* **57**, 1959-1967 (1989).
- 758 42. C. A. Buscaglia, O. Campetella, M. S. Leguizamon, A. C. Frasch, The repetitive domain  
759 of Trypanosoma cruzi trans-sialidase enhances the immune response against the catalytic  
760 domain. *J Infect Dis* **177**, 431-436 (1998).

- 761 43. A. F. Nardy, C. G. Freire-de-Lima, A. R. Perez, A. Morrot, Role of Trypanosoma cruzi  
762 Trans-sialidase on the Escape from Host Immune Surveillance. *Front Microbiol* **7**, 348  
763 (2016).
- 764 44. J. L. Affranchino, C. F. Ibanez, A. O. Luquetti, A. Rassi, M. B. Reyes, R. A. Macina, L.  
765 Aslund, U. Pettersson, A. C. Frasch, Identification of a Trypanosoma cruzi antigen that is  
766 shed during the acute phase of Chagas' disease. *Mol Biochem Parasitol* **34**, 221-228  
767 (1989).
- 768 45. N. Murphy, B. Rooney, T. Bhattacharyya, O. Triana-Chavez, A. Krueger, S. M. Haslam,  
769 V. O'Rourke, M. Panczuk, J. Tsang, J. Bickford-Smith, R. H. Gilman, K. Tetteh, C.  
770 Drakeley, C. M. Smales, M. A. Miles, Glycosylation of Trypanosoma cruzi TcI antigen  
771 reveals recognition by chagasic sera. *Sci Rep* **10**, 16395 (2020).
- 772 46. N. M. El-Sayed, P. J. Myler, D. C. Bartholomeu, D. Nilsson, G. Aggarwal, A. N. Tran, E.  
773 Ghedin, E. A. Worthey, A. L. Delcher, G. Blandin, S. J. Westenberger, E. Caler, G. C.  
774 Cerqueira, C. Branche, B. Haas, A. Anupama, E. Arner, L. Aslund, P. Attipoe, E.  
775 Bontempi, F. Bringaud, P. Burton, E. Cadag, D. A. Campbell, M. Carrington, J. Crabtree,  
776 H. Darban, J. F. da Silveira, P. de Jong, K. Edwards, P. T. Englund, G. Fazelina, T.  
777 Feldblyum, M. Ferella, A. C. Frasch, K. Gull, D. Horn, L. Hou, Y. Huang, E. Kindlund,  
778 M. Klingbeil, S. Kluge, H. Koo, D. Lacerda, M. J. Levin, H. Lorenzi, T. Louie, C. R.  
779 Machado, R. McCulloch, A. McKenna, Y. Mizuno, J. C. Mottram, S. Nelson, S. Ochaya,  
780 K. Osoegawa, G. Pai, M. Parsons, M. Pentony, U. Pettersson, M. Pop, J. L. Ramirez, J.  
781 Rinta, L. Robertson, S. L. Salzberg, D. O. Sanchez, A. Seyler, R. Sharma, J. Shetty, A. J.  
782 Simpson, E. Sisk, M. T. Tammi, R. Tarleton, S. Teixeira, S. Van Aken, C. Vogt, P. N.  
783 Ward, B. Wickstead, J. Wortman, O. White, C. M. Fraser, K. D. Stuart, B. Andersson,  
784 The genome sequence of Trypanosoma cruzi, etiologic agent of Chagas disease. *Science*  
785 **309**, 409-415 (2005).
- 786 47. J. V. Rajan, M. McCracken, C. Mandel-Brehm, G. Gromowski, S. Pollett, R. Jarman, J.  
787 L. DeRisi, Phage display demonstrates durable differences in serological profile by route  
788 of inoculation in primary infections of non-human primates with Dengue Virus 1. *Sci Rep*  
789 **11**, 10823 (2021).
- 790 48. W. Li, A. Godzik, Cd-hit: a fast program for clustering and comparing large sets of  
791 protein or nucleotide sequences. *Bioinformatics* **22**, 1658-1659 (2006).
- 792 49. L. Fu, B. Niu, Z. Zhu, S. Wu, W. Li, CD-HIT: accelerated for clustering the next-  
793 generation sequencing data. *Bioinformatics* **28**, 3150-3152 (2012).
- 794 50. M. Dysinger, L. E. King, Practical quantitative and kinetic applications of bio-layer  
795 interferometry for toxicokinetic analysis of a monoclonal antibody therapeutic. *J*  
796 *Immunol Methods* **379**, 30-41 (2012).

797

798 **Acknowledgments:** We thank members of the DeRisi Lab for helpful discussions during these  
799 studies. We also acknowledge the New York Blood Center for contribution of healthy  
800 control plasma. Contents herein are the sole responsibility of the authors and do not  
801 necessarily represent the official views of the NIH or other funding agencies.

## 802 **Funding:**

803 Chan Zuckerberg Biohub (JLD)

804 Chan Zuckerberg Biohub Physician-Scientist Fellowship Program (JDW)

805 National Heart Lung and Blood Institute award K38HL154203 (JDW)

806 **Author contributions:**

807 Conceptualization: JLD, JDW, CB, JVR

808 Methodology: JDW, JLD, CB, JVR, HMK, RJM, EDG, NLB, JJP, WW, RLT, SLS,  
809 EEO, JES, EHC, RHG, RC

810 Investigation: HMK, RJM, JDW, JVR, AM, NLB, GW, AM, AS, CJF, EAK, ET

811 Formal analysis: HMK, RJM, JVR

812 Visualization: HMK, RJM, JDW, JVR

813 Funding acquisition: JLD, JDW

814 Project administration: JDW, JLD

815 Supervision: JDW, JLD, CB, EDG

816 Writing – original draft: JDW, HMK, RJM

817 Writing – review & editing: All co-authors

818 **Competing interests:** JDW is a medical consultant for MelioLabs Inc. RJM is an employee of  
819 Agilent Technologies. HMK, RJM, JDW, CB, JVR, and JLD are inventors on a  
820 provisional patent application by the Regents of the University of California and the  
821 Chan Zuckerberg Biohub San Francisco that covers peptide antigens related to TS-2.23.  
822 The other authors declare that they have no competing interests.

823 **Data and materials availability:** All raw and processed data will be available for download on  
824 Dryad. PhIP-seq analytical code will be available at <https://github.com/hkortbawi>.